Article

Green Ceramic Machining: Determination of the Recommended Feed Rate for Y-TZP Milling

Anthonin Demarbaix [1,*], Marylou Mulliez [1,2], Edouard Rivière-Lorphèvre [1], Laurent Spitaels [1], Charles Duterte [2], Nicolas Preux [3], Fabrice Petit [3] and François Ducobu [1]

1 Machine Design and Production Engineering Unit, Faculty of Engineering, University of Mons, Place du Parc 20, 7000 Mons, Belgium; marylou.mulliez@alumni.umons.ac.be (M.M.); edouard.rivierelorphevre@umons.ac.be (E.R.-L.); laurent.spitaels@umons.ac.be (L.S.); francois.ducobu@umons.ac.be (F.D.)
2 Optec Laser Systems, Avenue des Nouvelles Technologies 53, 7080 Frameries, Belgium; charles.duterte@optec.be
3 Research and Technological Support Departement, Environmental Materials Research Association, INISMa, CRIBC, Avenue Gouverneur Cornez 4, 7000 Mons, Belgium; n.preux@bcrc.be (N.P.); f.petit@bcrc.be (F.P.)
* Correspondence: anthonin.demarbaix@umons.ac.be; Tel.: +32-65-375-040

Abstract: Manufacturing of advanced ceramic parts exhibiting complex geometries is laborious and expensive. Traditionally, the machining is carried out on a so-called 'green ceramic': a compact composed of ceramic powder held with the help of a binder. This difficulty is due not only to the composition of the material, but also to the lack of methods that determine optimal machining parameters. The goal of this paper is to apply the method based on ductile material behavior to determine a feed rate working range to ensure a machining quality. Indeed, a previous study demonstrated the limits of this method in determining cutting speed. In this case, two material removal mechanisms are observed: a mechanism dominated by pulling of the material and a proper machining mechanism. This demonstrates that the specific cutting energy is a reliable indicator for machining quality assessment. In the studied case, the recommended machining parameters to ensure quality machining of Y-TZP green ceramic with a 3 mm diameter cylindrical tool are: a cutting speed of 250 m/min, a feed per tooth of 0.037 mm/tooth, an axial depth of cut of 0.7 mm, and a radial depth of cut of 3 mm.

Keywords: green ceramic machining; milling; Yttria Tetragonal Zirconia Polycrystal Ceramic

1. Introduction

Advanced ceramics are mainly used in corrosive environments and high temperature applications compared to metals and polymers. Indeed, they exhibit high chemical inertia, and low thermal and electrical conductivities, while having interesting mechanical properties [1]. Ceramic materials can be made out of only one crystalline phase (homogeneous material) or out of many balanced crystalline phases (heterogeneous material) [2–4].

Ceramic material properties depend on the global chemical composition and the crystalline structure. This article focuses on the zirconium oxide ($ZrO2$), which is widely used in heat engines, the biomedical and food industries, and also in the luxury sector [1,5,6]. Zirconium oxide has several transformations on cooling from a molten state to room temperature; so-called polymorphic transformation. The three polymorphs are the monoclinic phase (stable up to 1170 °C), the tetragonal phase (stable between 1170 °C and 2370 °C) and the cubic phase (up to the melting point 2680 °C) [4]. The monoclinic-tetragonal transformation is martensitic, and is associated with a volumetric expansion of 3% to 5%. This transformation is based on the apparent displacive nature of the structural change that has invited the application of the theory of martensite crystallography to transformation. Reinforcement mechanisms for zirconium-based materials as $ZrO2$-toughened

ceramics (ZTC) is possible thanks to this martensitic transformation [7,8]. Moreover, the addition of Yttrium allows for stabilization of the tetragonal phase at ambient temperatures. The resulting material is called Y-TZP (Yttrium-stabilized Tetragonal Zirconia Polycrystal) and exhibits high mechanical properties: flexural strength of $900-1400$ MPa and fracture toughness of 5–9 MPa m$^{1/2}$ [9].

Ferraris et al. [1] demonstrate the traditional manufacturing chain which produces geometrically complex ceramic parts, and highlight that the last stage (finishing operations) represents 80% of the total part cost. Figure 1 shows the influence of process steps on the yield stress of an engineering ceramic with a toughness of 6 MPa m$^{1/2}$ such as Y-TZP. The major factor that considerably reduces the final properties of the part is the complex shaping step by machining, which generates microcracks ranging from 50 to 200 μm [10].
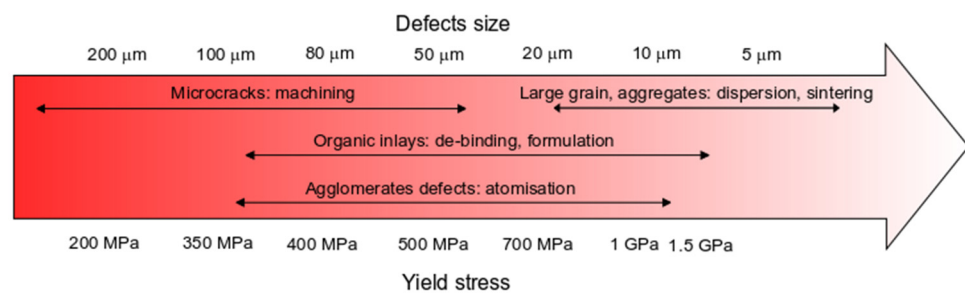

Figure 1. Evolution of yield stress in relation to the defect size for ceramic toughness of 6 MPa m$^{1/2}$.

Green Ceramic Machining (GCM) consists of machining the compacted ceramic powder held by a binder before the sintering operation [11]. GCM allows the ceramic to be machined while minimizing the risk of generating significant micro-cracks that can lead to premature failure of the ceramic part [9]. However, this traditional machining method is very laborious and relies essentially on the experience of the operator [1]. Moreover, no method is available to give optimal machining parameters to achieve the desired quality of machining.

Previous studies have shown that the behavior of the material during machining is different depending on the stage at which it is carried out in the production line [12]. The forces and energy during GCM are much lower than in polymer or metal machining. This is linked to the fact that the material removal process is mainly based on the separation mechanism of the binder and its load [13]. In fact, green machining is complex due to the pseudo-plastic fluid behavior of the binder [12]. Despite the increase of forces resulting from binder viscosity, the machining quality is not directly influenced by the rotational speed of the tool (i.e., the cutting speed). The arithmetic and total surface roughness remain constant whatever the cutting speed if the percentage of binder is above a threshold value [12,13]. Consequently, the roughness indicator alone does not allow a cutting speed to be recommended. Unfortunately, the tool–material Standard [14] also cannot be used to determine the recommended cutting speed because of the binder's behavior. The main required condition is to have a cutting speed fast enough to allow a permanent contact between the tangent edges of the tool and the material [12]. The cutting speed V_c (m/min) can be determined with the tool diameter D (mm) and the rotational speed of tool N (RPM) [15] by:

$$V_c = \frac{N \times D \times \pi}{1000} \tag{1}$$

Regarding the other machining parameter, the feed rate V_f (mm/min), which is the linear speed of the tool in the machining direction, is calculated [15] by:

$$V_f = N \times Z \times f_z \tag{2}$$

In this equation, f_z (mm/tooth) stands for the feed per tooth, N (RPM) the spindle speed and Z the number of teeth.

In the case of ductile materials, the tool–material coupling Standard [14] is used to establish recommendations for the operators. The recommendations of the machining parameters are given from the behavior of the material which is characterized using the specific cutting energy under predetermined conditions [14]. For determination of the feed rate, several slots are machined by varying this parameter and keeping the others constant. In fact, the range of chip thickness, which is a function of feed rate, is determined with the help of a graph which shows the specific cutting energy in relation to the chip thickness. In the slot case, the relation between chip thickness h (mm) and the feed per tooth is given for a cylindrical tool by:

$$h = f_z \tag{3}$$

The specific cutting energy W_c (W.min/cm^3) is the energy required to remove a unit of volume of material. This specific cutting energy can be calculated [14] by:

$$W_c = \frac{P_c}{Q} \tag{4}$$

Cutting power P_c (W) is the net power during the interaction of the tool with the material and Q (mm^3/min) stands for the machined material flow rate. The flow rate of the machined material Q is calculated for a cylindrical tool [14] by:

$$Q = \frac{N \times Z \times f_z \times a_p \times a_e}{1000} \tag{5}$$

With a_p (mm) and a_e (mm) which are the axial depth of cut and the radial depth of cut, respectively.

In the end, auxiliary parameters can be determined. These allow the definition of a model to evaluate the power generated by the cut. The auxiliary parameters $W_{c,ref}$ and correction coefficient m_c are calculated with the following model [9,14]:

$$W_c = W_{c,ref} \times \left(\frac{h_{ref}}{h}\right)^{m_c} \tag{6}$$

with $h_{ref} = h_{max}$ which is determined in the previous experiments.

The goal of this paper is to suggest a method to determine the recommended feed rate for the GCM of Y-TZP, and to obtain a model that would enable the control of the machining process based on the Standard.

2. Materials and Methods

2.1. Material

The Belgian Ceramic Research Centre manufactures green blanks of Y-TZP. The green body is composed of a fine Yttria Stabilized Zirconia powder (3 mol% yttria-TZ-3Y-SE-Tosoh Corporation, Tokyo, Japan) and an organic binder at 2 wt% (Zusoplast-Zschimmer and Schwartz, Lahnstein, Germany). According to the supplier, the actual particle size of powder is to around 10 nm with a specific surface area of 7 m^2/g.

A square blank of 70 mm side and 15 mm high is obtained by uniaxial compaction at 20 MPa followed by an isostatic compaction at 195 MPa for 5 min.

2.2. Methods

The experiments were carried out on a 3-axis machine-tool, which is a prototype manufactured by Optec laser systems, whose maximum spindle speed is 35,000 RPM. The carbide tool has a cylindrical shape of 3 mm with two teeth. The machining parameters are constant except for the feed per tooth (f_z). Table 1 shows the variation of feed per tooth (f_z) and the resulting feed rate (V_f). The variation of the feed rate was chosen according to the maximum speed capacity of the prototype axes of 4000 mm/min. The selected variation step was 200 mm/min. The other parameters were fixed at 0.7 mm for

the axial depth of cut (a_p), 3 mm for the radial depth of cut (a_e) and the spindle speed was set at 30,000 RPM.

Table 1. Fixed and varied parameters.

Parameters	Value									
Fixed parameters										
Z	2									
Tool diameter [mm]	3									
N [RPM] (or V_c[m/min])	30,000 (or 250)									
a_p[mm]	0.7									
a_e[mm]	3									
Varied parameters										
f_z [mm/tooth] / V_f[mm/min]	0.003 / 200	0.007 / 400	0.010 / 600	0.013 / 800	0.017 / 1000	0.020 / 1200	0.023 / 1400	0.027 / 1600	0.030 / 1800	0.033 / 2000
	0.037 / 2200	0.040 / 2400	0.043 / 2600	0.047 / 2800	0.050 / 3000	0.053 / 3200	0.057 / 3400	0.060 / 3600	0.063 / 3800	0.067 / 4000

Figure 2 shows the schematic configuration of the experimental setup. The square blank was fixed on a holder during the slots machining. The procedure recommended by the tool–material coupling Standard was followed. In particular, the Standard section which determined the operating range of the chip thickness. During each machined slot, the cutting power P_c was measured directly on the spindle (via acquisition of the current and the voltage of the axes) with the help of Aerotech software available on the machine-tool.
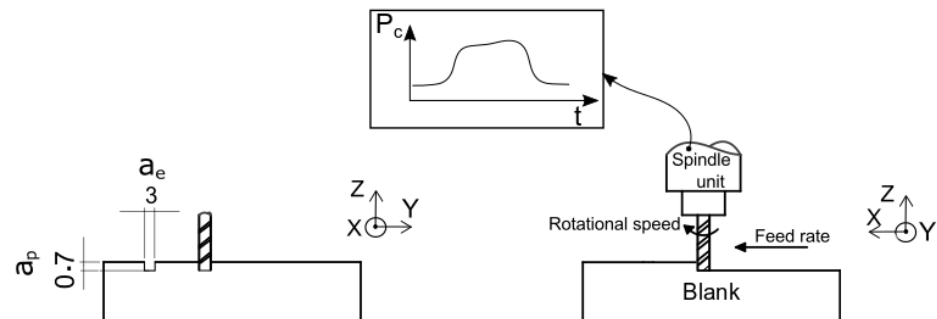

Figure 2. Schematic assembly of experimental setup (dimensions in mm).

The specific cutting energy (W_c) can be determined from this cutting power using the Equation (3) with P_c calculated by [14]:

$$P_c = P_{working} - P_{idling} \tag{7}$$

where $P_{working}$ is the power during the tool–material interaction and P_{idling} the power with no interaction between tool and material.

In addition to measuring the specific cutting energy, the standard requires visual observation of the machining quality to determine the minimum and maximum chip thickness values.

Roughness measurements (arithmetical R_a and maximum height R_z) for each slot were also carried out using an optical roughness meter (VK-X-Series Keyence, Itasca, IL, USA). The roughness measurement was carried out in three different areas of the slot over a 5 mm length with the "Multi-line Roughness" tool, which was used to determine the roughness from 21 profiles spaced of the few micrometers with a cutoff λ_c of 0.7 mm.

3. Results

Results are divided into three parts: visual observation, surface roughness and the specific cutting energy.

3.1. Visual Observation

A first visual observation, which can be seen in Figure 3, shows the appearance of striations at low feed rates and burr formation at the edge of the slots. The high stresses are mainly due to the entry of a tooth into the material. When the speed is lower, the tool will pull more of the material that is abrasive on the surface and thus generate higher forces. The higher the speed, the shorter the interaction time of the material with the tool tooth, resulting in machining without edge chipping. The passage of the tool defines circles on the machined surface that can be seen without the use of an optical instrument.
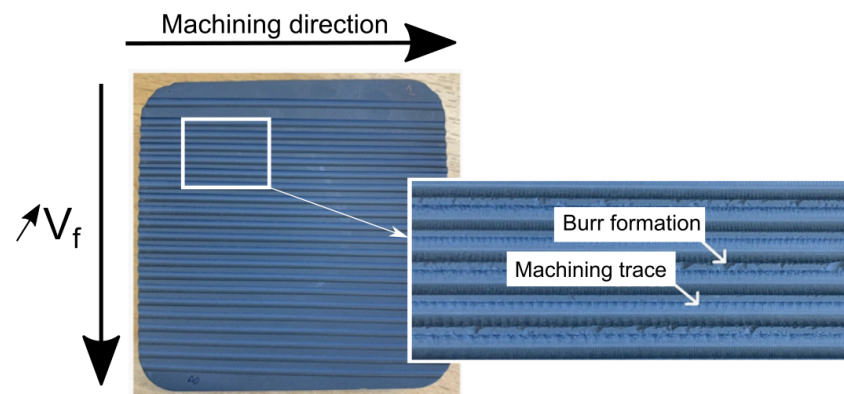
Figure 3. Visual observation of machining quality.

The surface analysis at the bottom of the slots in relation to the feed rate tends to support the above observation. Figure 4 also depicts two distinct zones with different topographies at the bottom of the slots. This shows that a threshold is visible on the roughness evolution. After this threshold feed rate, the surface topography shows traces of machining left during the tool passage, which characteristic of an end-milling operation. However, before this threshold, the tool does not leave any trace and an increase of craters is visible (in black). The size of these craters seems to decrease as the feed rate increases. This supports the previous statement that at low feed rates, the tooth will pull out the material causing significant damage on the machined surface.
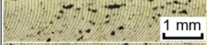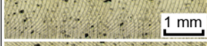
Before threshold			After threshold		
V_f [mm/min]	h [mm]	Machined surface view	V_f [mm/min]	h [mm]	Machined surface view
200	0.003		2200	0.037	
400	0.007		2400	0.040	
600	0.010		2600	0.043	
800	0.013		2800	0.047	
1000	0.017		3000	0.050	
1200	0.020		3200	0.053	
1400	0.023		3400	0.057	
1600	0.027		3600	0.060	
1800	0.030		3800	0.063	
2000	0.033		4000	0.067	

Figure 4. Machining quality at the bottom of the slots.

3.2. Surface Roughness

Figure 5 shows the evolution of the arithmetic roughness (R_a) and maximum height of roughness (R_z) in relation to the feed rate at constant depths of cut and cutting speed.

Figure 5. Roughness evolution in relation to the feed rate/chip thickness with the other parameters fixed (a spindle speed of 30,000 RPM, a radial depth of cut of 3 mm and an axial depth of cut of 0.7 mm).

The evolutions are identical for both R_a and R_z with two distinct zones: a first zone where the roughness is relatively variable around $R_{a,u}$ w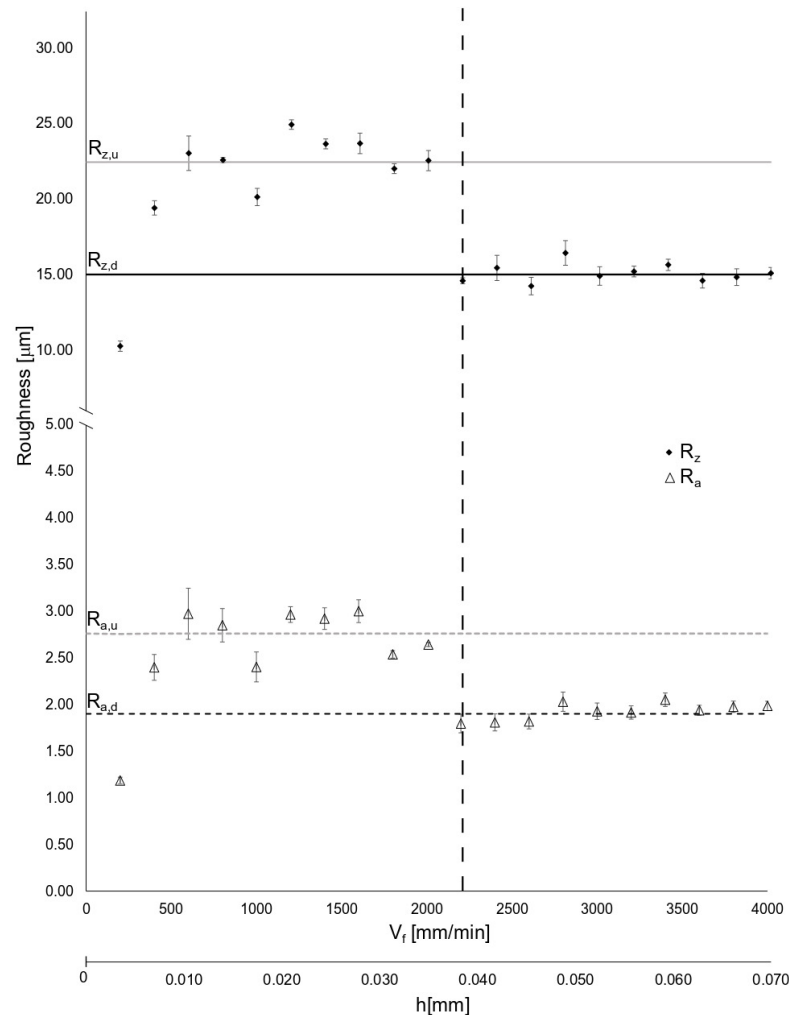ith a maximum R_a of 3 μm and around $R_{z,u}$ with a maximum R_z of 25 μm. After a chip thickness of 0.037 mm, the roughness drops to stabilize at an R_a value around 1.7 μm ($R_{a,d}$) and an R_z value around 15 μm ($R_{z,d}$).

3.3. Specific Cutting Energy

Figure 6 shows the evolution of the specific cutting energy in relation to the chip thickness (other parameters were kept constant). As the chip thickness increases, the specific cutting energy decreases with a stabilization for the last points despite the low forces. When the thickness of the chips is above a threshold value of 0.037 mm, a slight curve stall is visible. This leads after this threshold to a relative variation of the amplitude that does not exceed 5%.
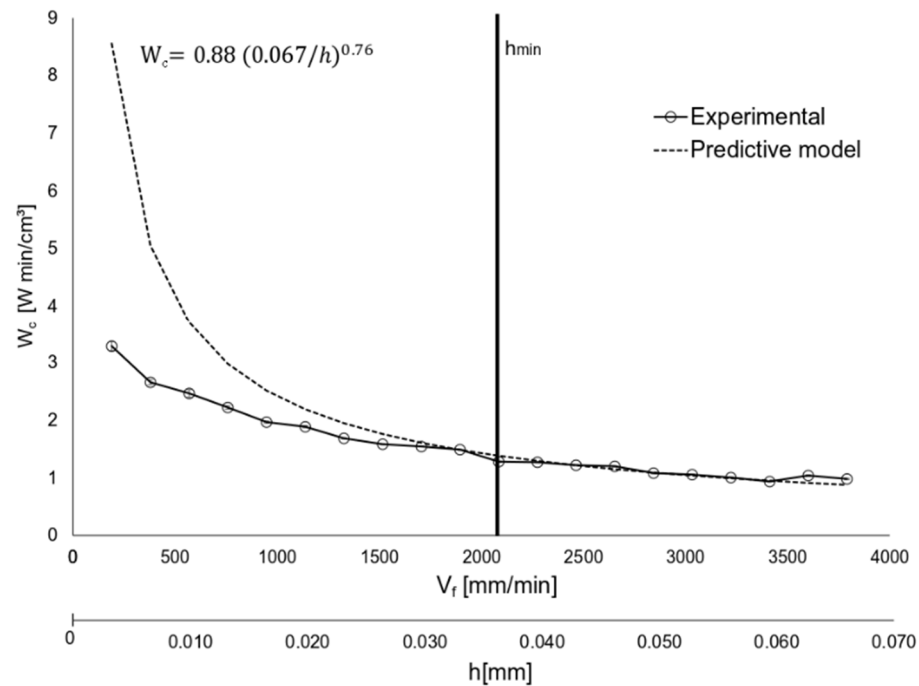
Figure 6. Evolution of specific cutting energy in relation to feed rate/chip thickness with other parameters fixed (a spindle speed of 30,000 RPM, a radial depth of cut of 3 mm and an axial depth of cut of 0.7 mm).

The model determined by following the Standard is:

$$W_c = 0.88 \times \left(\frac{0.067}{h} \right)^{0.76} \tag{8}$$

A break between the predictive and experimental curves is visible at a h_{min} of 0.037 mm. After h_{min}, the correlation coefficient R^2 is of 0.98. Finally, an operating range from h_{min} (0.037 mm) to h_{max} (0.067 mm, which is the limit capacity of the machine–tool) can be defined in which the variation of the specific cutting energy remains relatively stable at 1.05 W.min/cm^3. By plotting the curve determined according to the Standard, two distinct areas can be distinguished. On one hand, the curves are overlapped, thus showing that the model is predictive. On the other hand, a significant difference appears between the model and the experimental tests.

The specific cutting energy decreases as the feed rate increases, as observed by Onler et al. [13]. At constant cutting speed, the evolution of the specific cutting energy follows a behavior similar to a ductile material. As the tool speed remains unchanged, there is no influence on the rheology of the material which is mainly caused by the binder contained in the green compact. In addition, the threshold is the same as in the roughness analysis.

4. Discussion

The various results corroborate with those of Onler et al. [13]. Indeed, they revealed that the feed rate has an influence on the roughness and that the roughness improved as the feed rate increased. In addition, different results demonstrate that the threshold determines two distinct zones for both the specific cutting energy and the machining quality. A visual observation, whether with an optical instrument or not, makes the distinction of two zones possible. This distinction can be established by the trace left by the tool on the machined surface. Indeed, the two material removal mechanisms lead to this difference. These two different material removal mechanisms are a pull-out mechanism and a cutting mechanism. The first zone before a threshold is more of a material pull-out and therefore does not lead to a permanent contact between the tool and the material. This non-permanent contact will

result in a poor machining quality and accelerated tool wear. In addition, the burrs can be visualized easily, as mentioned by Onler et al. [13], and emphasizes the importance of the basic composition of the green ceramic blank [13]. Indeed, the choice of ceramic powder and binder influences the machining quality, as demonstrated by several authors [11,13,16]. This can have an impact on the blank, resulting in pores inside the material which will also play a role in the material properties. The craters formed by machining will have a negative impact on the mechanical properties of the material, as it could lead to accelerated crack propagation in the material.

However, in the second zone, the material removal mechanism is end-milling machining, in which the interaction between the tool and the material is permanent. The roughness analysis also significantly shows the two material removal mechanisms. This leads therefore to a machining operation that can be under control, also defining a recommended range for use from the roughness analysis. In addition, the roughness is relatively stable in this second zone.

The trend in specific cutting energy is like that reported by Onler et al. [13], with specific cutting energy increasing as the feed rate decreases [13]. In the end, the specific cutting energy is also a reliable indicator to determine a range of feed rates for a given spindle speed.

Finally, the threshold defined by each analysis is identical with a feed rate above 2200 mm/min, resulting in a chip thickness of 0.037 mm.

The application of the tool-material coupling Standard is therefore used to determine a recommended range of chip thickness values for GCM in an organically bound Y-TZP blank. In addition, determination of the auxiliary parameters is used to control the machining quality by giving an indication as to whether the material removal mechanism is machining or pull-out material. Finally, a procedure is proposed to assess the machining quality by monitoring the specific cutting energy. The first step is to detect the h_{min}, which can be carried out with a visual analysis. Then, the power cutting is measured for each slot by increasing the feed rate above the threshold at which the material removal mechanism is a machining mechanism. Finally, the predictive model is determined by calculating the specific cutting energy. The minimum points to be collected according to the Standard is four [14]. This predictive model can, for example, be used as a quality control chart.

5. Conclusions

In this paper, the study demonstrates that, when performing green ceramic machining of a Y-TZP blank, even though the cutting speed cannot be determined using the tool–material coupling Standard (because of the pseudo-plastic behavior of the binder), a part of the NF E 66-520-5 Standard can be used. In fact, the material behavior when the feed rate varies is similar to a ductile material, under the condition that the spindle speed remains fixed. The specific cutting energy is therefore a reliable indicator to determine an operating range of the chip thickness. In addition, auxiliary parameters can be determined by following the Standard, and provides a model to predict the cutting power required to ensure optimum machining quality. Indeed, two distinct areas are highlighted during the GCM: an area where the material removal mechanism is a pull-out and an area where the mechanism is a cutting mechanism. This has a direct impact on the surface quality obtained by machining, and defines two distinct areas of surface roughness. This indicator can therefore be used as a quality indicator by ensuring that the specific cutting energy measured is on the previously determined theoretical curve.

Recommended cutting parameters are a feed rate greater than 2200 m/min for a depth of cut of 0.7 mm, a radial depth of cut of 3 mm for a cylindrical tool of diameter 3 mm with a spindle speed of 30,000 RPM. These machining parameters will result in a R_a value around 1.7 μm and a R_z value around 15 μm.

Conflicts of Interest: The authors declare no conflict of interest.

References

1. Ferraris, E.; Vleugels, J.; Guo, Y.; Bourell, D.; Kruth, J.-P.; Lawers, B. Shaping of engineering ceramics by electro, chemical and physical processes. *CIRP Ann.—Manuf. Technol.* **2016**, *65*, 761–784. [CrossRef]
2. Wongkamhaeg, K.; Dawson, D.V.; Holloway, J.A.; Denry, I. Effect of Surface Modification on In-Depth Transformations and Flexural Strength of Zirconia Ceramics. *J. Prosthodont.* **2018**, *28*, e364–e375. [CrossRef] [PubMed]
3. Gremillard, L. *Biocéramiques: Des Monolithes Aux Composites*; HDR Report; INSA de Lyon, Université Claude Bernard-Lyon I: Villeurbanne, France, 2009.
4. Murphy, W.; Black, J.; Hastings, G. *Handbook of Biomaterial Properties*; Springer: New York, NY, USA, 2016.
5. Kuebler, J.; Blugan, G. Failure analysis of zirconia ceramic watch bracelet. *Eng. Fail. Anal.* **2011**, *18*, 625–632. [CrossRef]
6. Bilal, A.; Jahan, M.P.; Talamona, D.; Perveen, A. Electro-Discharge Machining of Ceramics: A review. *Micromachines* **2019**, *10*, 10. [CrossRef]
7. Brog, J.-P.; Chanez, C.-L.; Crochet, A.; Fromm, K.M. Polymorphism, what it is and how to identify it: A systematic review. *RSC Adv.* **2013**, *3*, 16905–16931. [CrossRef]
8. Hannink, R.H.J.; Kelly, P.M.; Muddle, B.C. Transformation Toughening in Zirconia-Containing Ceramics. *J. Am. Ceram. Soc.* **2004**, *87*, 461–487. [CrossRef]
9. Demarbaix, A.; Rivière-Lorphèvre, E.; Ducobu, F.; Filippi, E.; Petit, F.; Preux, N. Behaviour of pre-sintered Y-TZP during machining operations: Determination of recommended cutting parameters. *J. Manuf. Process.* **2018**, *32*, 85–92. [CrossRef]
10. Sannon, C. Lumière Sur La Zircone 3Y-TZP Utilisée en Implantologie Orale: Étude de La Relation Entre La Microstructure et La Durabilité. Ph.D. Thesis, INSA de Lyon, Université de Lyon,, Lyon, France, 2015.
11. Easler, T.E.; Khalfalla, Y.; Benyounis, K.Y. Green Machining. In *Reference Module in Materials Engineering*; Elsevier: Amsterdam, The Netherlands, 2016; pp. 6–8.
12. Demarbaix, A.; Ducobu, F.; Preux, N.; Petit, F.; Rivière-Lorphèvre, E. Green Ceramic Machining: Influence of the Cutting Speed and the Binder Percentage on the Y-TZP Behavior. *J. Manufuf. Mater. Process.* **2020**, *4*, 50. [CrossRef]
13. Onler, R.; Korkmaz, E.; Kate, K.; Chinn, R.; Are, S.; Ozdoganlar, O.B. Green micromachining of ceramics using tungsten carbide micro-endmills. *J. Mater. Process. Technol.* **2019**, *267*, 268–279. [CrossRef]
14. Association Française de Normalisation AFNOR (1999)—NF E 66-520-5 (E). *Working Zones of Cutting Tools—Part 5: Application to Milling Technology*; AFNOR Group: La Plaine Saint-Denis, France, 1999.
15. Altintas, Y. *Manufacturing Automation: Metal Cutting Mechanics, Machine Toolvibrations, and CNC Design*; The Press Syndicate of the University of Cambridge: Cambridge, MA, USA, 2000.
16. Dhara, S.; Su, B. Green Machining to Net Shape Alumina Ceramics Prepared Using Different Processing Routes. *Int. J. Appl. Ceram. Technol.* **2005**, *2*, 262–270. [CrossRef]